Arterial segmentation and visual stimulus-induced changes in diameter observed in the human brain

Alexandre Bizeau[1,2], Guillaume Gilbert[3], Minh Tung Huynh[4], Michaël Bernier[1,2], Christian Bocti[5], Maxime Descoteaux[2,6], and Kevin Whittingstall[1,2,4]

[1]Department of Radiation Sciences and Biomedical imagery, Université de Sherbrooke, Sherbrooke, QC, Canada, [2]Centre d'Imagerie Moléculaire de Sherbrooke (CIMS), Centre de Recherche CHUS, Sherbrooke, QC, Canada, [3]MR Clinical Science, Philips Healthcare, Markham, ON, Canada, [4]Department of Diagnostic Radiology, Université de Sherbrooke, Sherbrooke, QC, Canada, [5]Department of Medecine, Université de Sherbrooke, Sherbrooke, QC, Canada, [6]Department of Computer Science, Université de Sherbrooke, Sherbrooke, QC, Canada

Synopsis

When undergoing stimulation, neurons need to be supplied with oxygen and glucose. This demand then induces vasodilation generated by the astrocytes which act on the muscles of the arteries of the human brain. Using time-of-flight magnetic resonance angiography acquisitions, we extracted the apparent diameter of arterial vessels. We then compared diameter with and without visual stimulation and demonstrated that smaller vessels dilate proportionally more than larger ones in the posterior cerebral arteries. Using this method, the investigation of the coupling between neural activity and regional cerebral vasodilation, also called functional hyperhemia, is now possible.

Introduction

The diameter of cerebral vessels is dynamic and thought to be mediated by neural and astrocytes signaling[1]. While several studies in animal models have reported stimulus-induced vasodilation, measuring this in humans is not straightforward[2], although this could provide important information on neurovascular coupling. Here, we report on a novel and non-invasive MRI approach for quickly assessing changes in cerebral arterial diameter, which is then used to study the arterial response of the visual cortex, perfused by the posterior cerebral arteries (PCA[3])

Material and Methods

All MRI images were acquired on 4 healthy subjects at the Sherbrooke University Hospital Center (CHUS) using an Ingenia 3T Philips scanner. A low-resolution, 4-chunk, full brain time-of-flight (ToF[4]) (200 slices, TR/TE/Flip angle=23ms/3.6ms/18^{o}, 512x512x200 reconstructed voxels, acquisition resolution of 0.5x0.5x1.2mm, reconstructed resolution of 0.5x0.5x0.6mm, 2min acquisition time) was acquired as a scout to identify the PCA. Once the location of these arteries was determined, two high-resolution ToF with only one chunk (100 slices, TR/TE/Flip angle=23ms/3.6ms/18^{o}, 0.3mm isotropic reconstructed resolution, 5m45s acquisition time) were acquired in the same region: we first acquired a 'resting state' ToF where the subject had their eyes closed with the lights turned off. A second ToF was acquired while the subject viewed an action movie containing several scene cuts and contrast changes (no sound);

Figures

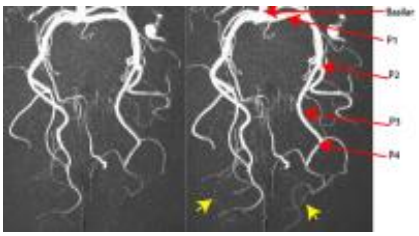

Comparison of MIP of two time-of-flight angiographies: resting-state (left) and with visual stimulation (right). We can clearly see that new vessels become visible near the visual cortex (short arrows). Those vessels were too small to appear on the resting-state angiography due to the image resolution. Long arrows indicate vessel sections.

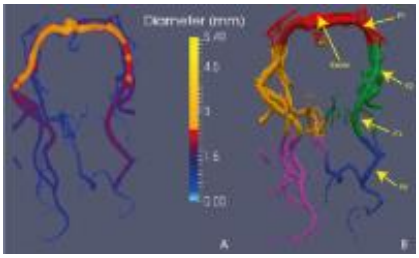

A) A vessel segmentation and diameter extraction on the posterior cerebral arteries (PCA). B) Example of the sub-division into five clusters which are Basilar with P1. For left and right, P2-P3 are grouped and P4 with smaller vessels. Image represents a part of the basilar and leading to the P4.

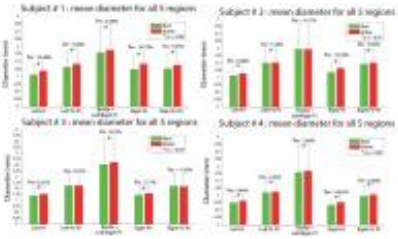

Graph comparing the mean diameter of resting-state and stimulation in each 5 regions. Error-bar shows the standard deviation between vessel calibers in the region. Representations are for all 4 subjects.

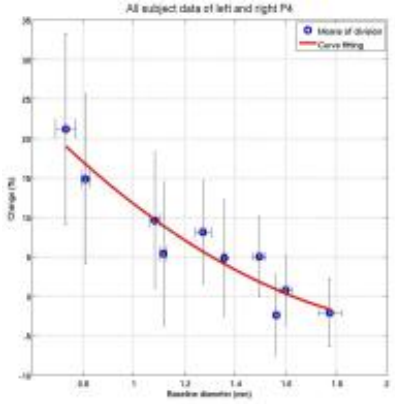

Graph representing the percentage change $(D - D_0)/D_0$ on y-axis and the resting-state

both known to reliably activate visual neurons[5]. Compared to typical visual stimuli (i.e. checkerboards), this is advantageous to minimize subject fatigue given the relatively long stimulation period.

Pre-processing consisted of a registration of the two ToF followed by skull stripping with FSL's BET and denoising by a non-local means via Dipy. For vessel segmentation, our method is based on Hessian-based vesselness measure[6]. Briefly, bright tubular structures are identified, segmented and stored for further analysis. We used vessel enhancing diffusion (VED[7]) to smooth the vessels and removes noise from the segmentation. To estimate diameter, a local thickness technique[8] was performed by fitting the largest sphere in the segmentation binary mask. This resulted in a voxel-based diameter measure along each segmented vessel. Once segmented, the PCA was manually classified into their corresponding known sections (Basilar, P1, P2, P3, P4) by a radiology resident, which were then classified into five different clusters of similar sizes. A two sample paired t-test was used to assess significant differences in diameter between resting and activated states. For that, we computed the percentage change $(D - D_0)/D_0$, where D is the diameter of an active voxel and D_0 is the diameter of the same voxel in the rest image.

Result and Discussion

An example of a resting and active ToF maximum intensity projection (MIP) from one subject is shown in Figure 1. Clearly, stimulation enhanced the visibility of small vessels near the posterior portion of the occipital lobe; it can be seen by counting the number of new voxels in the active segmented image (~10.62±4.45%). A 3D reconstruction of the PCA, color-coded for diameter, along with the cluster classification used for computation is shown in Figure 2. Average apparent diameter values for all five PCA regions in rest and stimulus conditions are shown in Figure 3 for each participant (N=4).

In each subject (N=4), with stimulus-evoked a change in caliber was observed everywhere[9], but there is a greater vasodilation in small vessels. This is evident when pooling data across all subjects and voxels spanning P4 and binning baseline diameter values in 10% increments (Figure 4). On average, stimulation dilated vessels in the 0.8mm range by ~20%, those around 1.6mm remained unchanged and vessels larger than 1.8mm appeared to constrict. In each subject, we found that around 57.44±16.04% of voxels dilate, 31.75±11.81% remain invariant and 10.81±6.25% constrict (Figure 5).

In summary, our data indicate that visual stimulation increases the apparent arterial diameter in the majority of the PCA. Such vasodilation is particularly strong in the smaller vessels near the cortex, in line with findings observed in animal models[10]. However, with the present data, we

baseline diameter in millimeter on x-axis. Data was pooled across all subjects for all voxels spanning P4 (left and right) and binned as 10% increments for baseline diameter values.

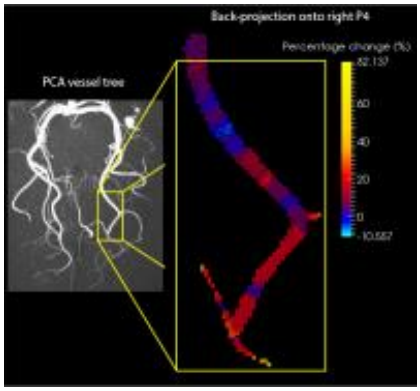

Back-projection of the percentage change $(D - D_0)/D_0$ onto the corresponding voxel. Left: MIP of the ToF. Right: sub-division of the right P4 of subject #1.

cannot rule out that the observed vasodilation results from enhanced image contrast (i.e. due to increased blood flow) rather than a true increase in diameter and we must take into account the partial volume effect, some vessels are not larger than the image resolution. We are currently acquiring measures of cerebral blood flow (CBF) to investigate this, as well as stimulus-evoked susceptibility weighted with phase difference (SWIp[11]) acquisitions to confirm that venous dilation is indeed smaller than arterial dilation, as suggested in previous animal model studies[10]. Finally, we are currently experimenting with faster ToF acquisitions in order to measure the dynamic changes in vessel diameter on shorter time scales.

Acknowledgements

No acknowledgement found.

References

1. Koehler, R. C., Gebremedhin, D. & Harder, D. R. Role of astrocytes in cerebrovascular. 100, 307–317 (2006).

2. Hua, J. et al. Inflow-based vascular-space-occupancy (iVASO) MRI. Magn. Reson. Med. 66, 40–56 (2011).

3. Bell, R., Severson, M. A. & Armonda, R. A. Neurovascular Anatomy: A Practical Guide. Neurosurg. Clin. N. Am. 20, 265–278 (2009).

4. Dumoulin, C. & Jr, H. H. Magnetic resonance angiography. Radiology MI-5, 140–151 (1986).

5. Whittingstall, K., Bartels, A., Singh, V., Kwon, S. & Logothetis, N. K. Integration of EEG source imaging and fMRI during continuous viewing of natural movies. Magn Reson Imaging 28, 1135–1142 (2010).

6. Descoteaux, M. A Multi-Scale Geometric Flow for Segmenting Vasculature in MRI: Theory and Validation. (2004).

7. Manniesing, R., Viergever, M. a. & Niessen, W. J. Vessel enhancing diffusion. A scale space representation of vessel structures. Med. Image Anal. 10, 815–825 (2006).

8. Dougherty, R. & Kunzelmann, K.-H. Computing Local Thickness of 3D Structures with ImageJ. Microsc. Microanal. 13, 1678–1679 (2007).

9. Faraci, F. M. & Heistad, D. D. Regulation of large cerebral arteries and cerebral microvascular pressure. Circ. Res. 66, 8–17 (1990).

10. Huo, B.-X., Gao, Y.-R. & Drew, P. J. Quantitative separation of arterial and venous cerebral blood volume increases during voluntary locomotion. Neuroimage 105, 369–379 (2015).

11. Chen, Z., Gilbert, G. & Fuderer, M. Improved contrast in multi-echo susceptibility-weigthed imaging by using non-linear echo combination. Proc. ISMRM 23, 1730 (2015).